CHARACTERISATION OF SILVER THICK-FILM CONTACT FORMATION ON TEXTURED MONOCRYSTALLINE SILICON SOLAR CELLS

S. Kontermann, G. Emanuel, J. Benick, R. Preu, G. Willeke
Fraunhofer Institute for Solar Energy Systems (ISE)
Heidenhofstrasse 2, D-79110 Freiburg, Germany
phone: +49 (0)761–4588–5197, fax: +49 (0)761–4588–9250
e-mail: stefan.kontermann@ise.fraunhofer.de

ABSTRACT: The investigations presented in this paper help to clarify the firing temperature dependence of the microstructure at the interface of Ag thick-film contacts on textured silicon solar cells. Textured silicon wafers were chosen to put the investigations in a more relevant environment of a real solar cell. Scanning Electron Microscope (SEM) pictures were taken from silicon wafer surfaces beneath the contact where we found bright and dark regions. We identified them as the SiN layer deposited as an antireflection coating before printing and pure silicon originating from the raw wafer where the SiN layer was completely etched by the glass frit. The percentage of the surface area of the dark regions was quantified and brought into relation with the measured electrical properties and the recorded specific contact resistance. A clear correlation could be shown. The results are discussed referring to models of charge carrier transport in thick-film contacts.
Keywords: Contact, Modelling, Screen Printing, Microstructure

1 INTRODUCTION

The silver thick-film technology is predominantly used for contacting the n^+-emitter of industrial crystalline silicon solar cells [1]. One limiting parameter to the efficiency of the solar cell is the contact resistivity ρ_C. In order to achieve lower ρ_C a profound understanding of the contact is necessary.

The contact forms during a high temperature step while the cell is fired at temperatures of 700°C-860°C after printing and drying the silver paste. Parameters that influence the contact formation are the characteristics of the SiN_x antireflection coating, the emitter doping profile, the temperature time profile and the gas atmosphere during fast firing, the surface of the solar cell, i.e. the texture, the composition of the metal paste and its glass frit.

The glass frit plays an important role for the mechanical and electrical contact formation. In the high temperature step the glass frit enhances the sintering of the silver particles, wets and etches the SiN antireflection coating. The formation of cavities in the underlying silicon is explained by two different approaches:

- Si dissolves in a liquid lead-silver phase [2]
- The glass frit etches the silicon surface anisotropically [3]

While cooling down, silver recrystallises in these cavities and the characteristic silver crystallites grow on the silicon surface [4]. The glass frit solidifies as well and forms a layer of unknown – but probably low – conductivity near the silicon surface isolating some of the crystallites from the silver bulk.

So far, studies investigated the nature of these contacts on planar silicon wafers. We present experiments that were carried out on textured silicon solar cells, as this is closer to a real solar cell.

SEM studies were performed and are discussed in point of view of contact formation and especially the specific contact resistance.

To evaluate the contact formation and to asses the potential of reducing the contact resistivity we varied the peak firing temperature.

2 EXPERIMENTAL

2.1 Solar cell fabrication

[100] oriented 125×125 mm^2 Cz-Si wafers of 240 µm thickness (p-type 0.5-1.7 Ωcm) were etched in a dilution of potassium hydroxide (KOH) and isopropanol (IPA) to yield a texture of random pyramids with a maximum height of 12 µm. The wafers were diffused at approximately 850°C to give a sheet resistance R_{SH} of 45 Ω/sq. and a maximum typical near-surface doping concentration of about $N \sim 7{,}5 \times 10^{20}$ cm^{-3} (measured by SIMS). After phosphosilicate glass removal, a layer of sputtered SiN_x with a thickness of 70 nm was deposited on the wafers. Commercially available thick-film aluminium and two silver pastes (referred to as batch 1 and batch 2) were screen-printed and dried at 260°C for approximately 10 minutes. The samples were fired at peak temperatures in the range 740°C – 820°C (batch 1) and 700°C – 860°C (batch 2) using Rapid Thermal Firing [5]. A pyrometer was used for fast and exact temperature control. Finally the cells were edge isolated by a laser.

After electrical characterisation the solar cells were cut into appropriate pieces for further characterisation with SEM and specific contact resistivity measurements using the transmission line model (TLM).

2.2 Preparation of SEM samples

2×2 cm^2 pieces were cut out of the fabricated cells. To obtain access to the contact interface, these pieces were chemically etched by a HNO_3 – HF – HNO_3 – HF sequence including rinsing steps in between. A 70% HNO_3 solution at 80 °C was used to remove the silver. The etching time was 10 minutes. The glass in the fired fingers was etched by a 1% HF solution at room temperature for 4 minutes. During the HNO_3 etch, the silicon surface is covered by SiO with the thickness of some atomic layers. The subsequent HF etch removes this layer. Silicon is nearly not affected by the HF etch: a 48% HF dilution etches silicon with the rate of 0.03 nm/min [6]. So in the worst case the surface is etched in the dimensions of angstrom and will hence not influence the results significantly.

3 CHARACTERISATION BATCH 1

3.1 Solar cell parameters

Illuminated I-V-characteristics were measured. The series resistance $R_{s\text{-}light}$ was taken as proposed by [7]. Results are shown in figure 1.

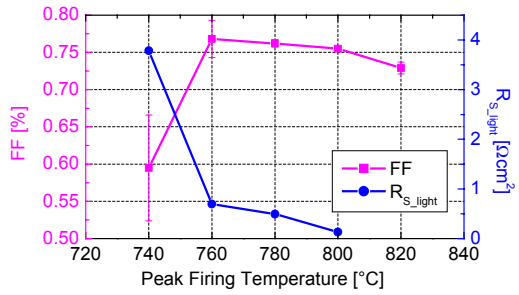

Figure 1: Fillfactor and series resistance $R_{s\text{-}light}$.

The fillfactor is best for 760°C with 76.8%. This is due to a heavily reduced series resistance $R_{s\text{-}light}$ from 760°C upwards. The fillfactor is slightly decreasing above 760°C due to increased space charge recombination. Efficiencies reached values up to 17.1%.

3.2 Formation of the contact on texturised solar cells

Figure 2 shows the contact interface after contact removal for different firing temperatures for batch 1.

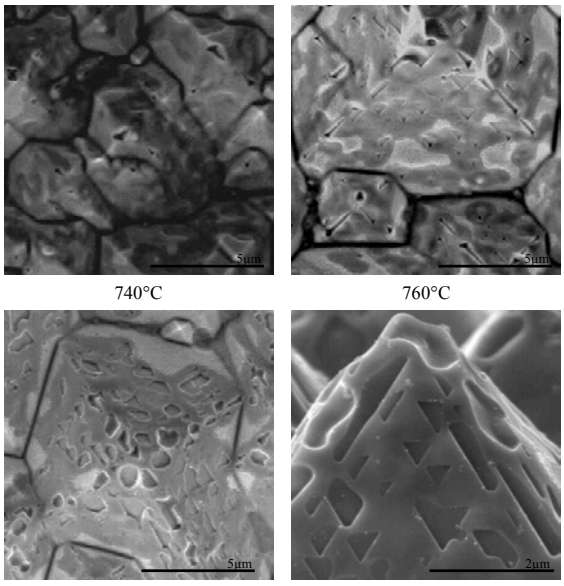

Figure 2: Development of imprints on random pyramids with increasing peak firing temperature.

When firing the silver paste, contact formation takes place by the glass frit etching through the SiN antireflection coating and silver crystals growing into the silicon. Contact formation is described as follows:

At the lowest peak firing temperature of 740°C, we observed that the random pyramids are mainly affected at their tip. Here we found their top being taken away and a triangular cavity of a former silver crystallite.

For 760°C the imprints on top tend to enlarge and stretched imprints form at the edge of the pyramids. At this temperature a new mechanism is launched and imprints emerge on the side surface of the random pyramids. These imprints have the shape of triangles that point towards the base of the random pyramids. These triangular imprints are not as deep as the imprints on top of the random pyramids and on the edges of the pyramids.

At 800°C the imprints on the side surface grow deeper and partially enlarge and loose their triangular shape. The imprints at the edges and on top of the random pyramids deepen significantly. The last SEM picture in figure 2 shows a side view of a random pyramid with the triangular imprints.

We explain the formation of the triangular imprints as follows: On planar [100] oriented Si wafers, cavities on the Si surface develop during firing and have the form of inverted pyramids. The side faces of these inverted pyramids are {111} planes [2]. The side faces of the pyramids created during texturing are as well {111} planes. Hence the development of inverted pyramids on a surface with texture pyramids will result in an imprint of the side face of an inverted pyramid on the texture pyramid. And this is just a triangle pointing downwards.

All SEM-pictures allow to distinguish bright and dark regions on the random pyramids. We observed that the imprints only appear in the dark regions.

4 CHARACTERISATION BATCH 2

All parameters shown for batch 2 are taken from the best cell out of three identically processed wafers.

4.1 Solar cell parameters

The same measurements as in 3.1 were performed and are shown in figure 3.

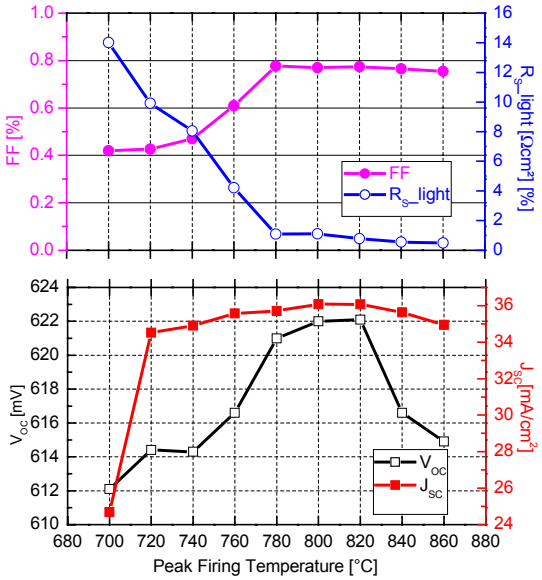

Figure 3: Solar cell parameters taken from the best cell at each firing temperature.

The processed cells show reasonable fillfactors from 780°C upwards. At 780°C the fillfactor reaches its maximum value of 77.7%. The measured series resistance is dropping for increasing firing temperatures and reaches at 780°C a low value of $R_{s\text{-}light} = 0.49\ \Omega cm^2$ allowing the fillfactor to rise. The short circuit current is

best at 820°C while the fillfactor is still on a high level and hence the best performing cell with the highest efficiency of 17.4% was fired at this temperature.

4.2 TLM measurements

We extracted a piece of 1×5 cm^2 from the solar cells to obtain a test structure to evaluate the specific contact resistance ρ_C according to the TLM as proposed by Berger [8] and reviewed by Reeves [9]. Figure 4 shows the results.

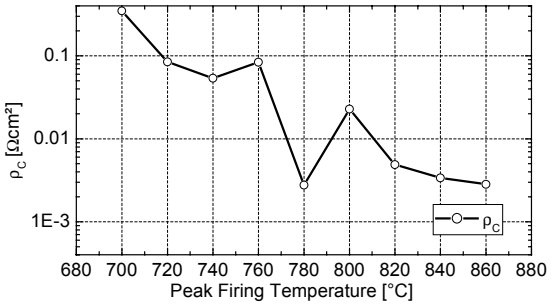

Figure 4: Specific contact resistance ρ_C measured using the transmission line model.

The specific contact resistance is in principal diminishing for increasing temperature. It is interesting that at 760°C ρ_C is slightly rising then dropping significantly at 780°C and increasing again at 800°C before it reduces constantly for higher temperatures. A specific contact resistance of good quality ($\rho_C < 3\times10^{-3}$ Ωcm²) is obtained from 780°C upwards except for 800°C where $\rho_C = 2\times10^{-2}$ Ωcm².

4.3 SEM studies on the microstructure

The following pictures in figure 5 describe the evolution of the contact interface with increasing peak firing temperature on a microscopic scale.

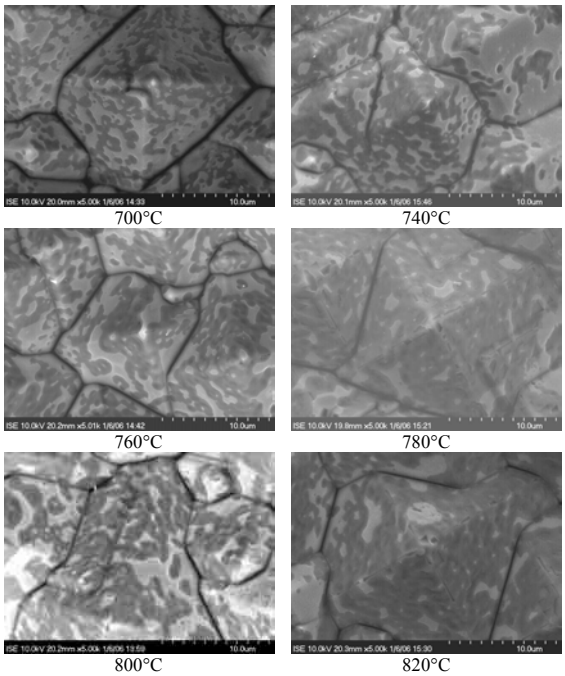

Figure 5: SEM pictures showing the evolution of the contact interface for an increasing firing temperature.

One can see from the pictures that for this paste, imprints exist for 780°C and 820°C on the edges and on top of the pyramids. Clear imprints on the side surfaces were not found. Bright and dark regions are again distinguishable. For an increasing peak firing temperature the dark regions tend to enlarge.

EDX studies in figure 6 show that a bright region (spectrum 1) contains a significant amount of nitrogen, while the same measurement on a dark region (spectrum 2) detects nearly no nitrogen.

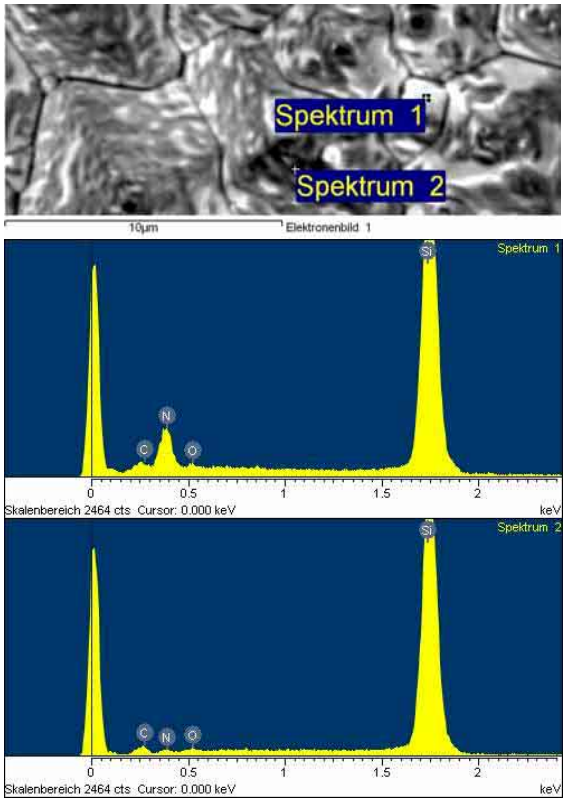

Figure 6: EDX spectra taken on a bright (1) and dark (2) region showing a significant nitrogen content for the bright appearing region (spectrum 1).

From these results we deduce that bright regions represent the SiN antireflection coating and that the dark regions correspond to a region where the glass frit etched the SiN antireflection coating and revealed the underlying silicon. As for an increasing peak firing temperature a different amount of dark surface is visible in figure 5, the assumption of a temperature dependent etching of the glass frit is supported.

As stated above, we found imprints of crystallites for 780°C and 820°C, but the solar cells show a non-vanishing fill factor for the other temperatures as well. This suggests that current flow is not only connected to the crystallites. As the dielectric SiN is an insulating layer, we suppose that current flow is only possible across the dark regions, whether there are crystallites or not.

4.4 Correlation of specific contact resistance and dark regions

We looked for a correlation between the surface area of dark regions and the specific contact resistance ρ_C and

expect a negative correlation between these quantities.

With an image editing program we segmented the pictures in white and black and calculated with this program the appropriate surfaces to obtain the fraction of dark surface. The graphical process is shown in figure 7.

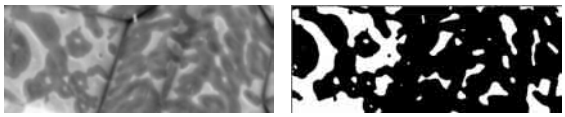

Figure 7: Segmentation of the SEM pictures into black and white.

The fact that in reality the surfaces are sides of pyramids and are pressed in plane by segmenting should be negligible, as both – dark and bright regions – are pressed in plane.

This evaluation was carried out for SEM pictures of samples for peak firing temperatures up to 820°C. The results are shown in figure 8 together with the appropriate specific contact resistance.

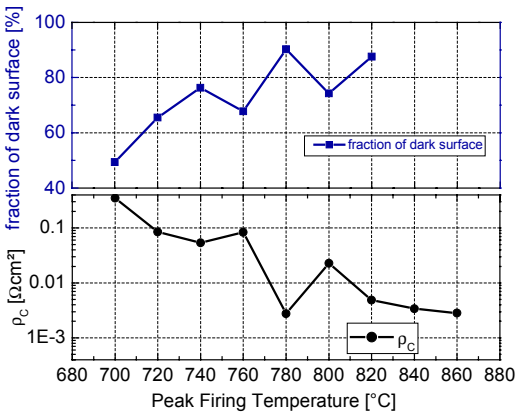

Figure 8: Comparison of the fraction of dark surface area with the specific contact resistance.

One can see from the graph that the fraction of dark surface lies between 45% and 90%. With increasing peak firing temperature the fraction increases in the range 700°C - 740°C to 78%, falls to 68% at 760°C and increases at 780°C to its highest value of 90%.

The curve of ρ_C develops with increasing firing temperature inversely. The lowest specific contact resistance is obtained at 780°C with $\rho_C = 2.77 \times 10^{-3}$ Ωcm². This result supports the hypothesis that the specific contact resistance correlates to the dark surface regions.

4.5 Discussion

The model for planar wafers proposed of Grupp et al. in [10] has shown a good performance. In our case the imprints of silver crystallites were found in batch 1. They were not accessible by an atomic force microscope, because the silicon surface with its random pyramids of 12 µm height was too rough. In batch 2 crystallites were found only for 780°C and 820°C. Further investigations are necessary to clarify, if it is sufficient to evaluate dark regions to calculate the specific contact resistance as this would represent an easier way than counting single crystallites.

5 CONCLUSION

Silicon solar cells were processed and fired at different peak temperatures. Illuminated and dark I-V-curves were measured. SEM studies on the interface of the silver thick-film contact revealed a firing temperature dependence. Beneath the contact we found two different regions. One where the SiN from the antireflection coating still covered the silicon and another where the SiN was etched away by the glass frit of the paste.

Regions without a remaining SiN layer were quantitatively measured. A correlation between an increasing surface without SiN layer and a decreasing specific contact resistance was found. Further investigations are necessary to clarify if the consideration of surfaces is sufficient for specific contact resistance calculation.

6 ACKNOWLEDGEMENT

The authors would like to thank E. Schäffer for measurements and A. Leimenstoll for emitter diffusion. This work was supported by the Stiftung der Deutschen Wirtschaft and the Freiburger Materialforschungs-zentrum.

7 REFERENCES

[1] J. F. Nijs, J. Szlufcik, J. Poortmans et al., IEEE Trans. Electron Devices 46 (1999) 1948.

[2] G. Schubert, F. Huster, and P. Fath, Proceedings of the 19th European Photovoltaic Solar Energy Conference, Paris, France (2004) 813.

[3] C. Ballif, D. M. Huijic, A. Hessler-Wyser et al., Proceedings of the 29th IEEE Photovoltaics Specialists Conference, New Orleans, Louisiana, USA (2002) 360.

[4] C. Ballif, D. M. Huljic, G. Willeke et al., Appl. Phys. Lett. 82 (2003) 1878.

[5] D. M. Huljic, D. Biro, R. Preu et al., Proceedings of the 28th IEEE Photovoltaics Specialists Conference, Anchorage, USA (2000) 379.

[6] Hull, Properties of Crystalline Silicon (INSPEC, London, 1999).

[7] A. G. Aberle, S. R. Wenham, and M. A. Green, Proceedings of the 23rd IEEE Photovoltaic Specialists Conference, Louisville, Kentucky, USA (1993) 133.

[8] H. H. Berger, IEEE International Solid-State Circuits Conference, (1969) 160.

[9] G. K. Reeves and H. B. Harrison, IEEE Electron. Dev. Lett. EDL-3 (1982) 111.

[10] G. Grupp, D. M. Huljic, R. Preu et al., Proceedings of the 20th European Photovoltaic Solar Energy Conference, Barcelona, Spain (2005).